NASA Technical Memorandum 109011

A Decoupled Control Approach for Magnetic Suspension Systems Using Electromagnets Mounted in a Planar Array

Nelson J. Groom

August 1993

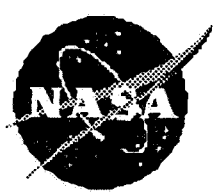

National Aeronautics and
Space Administration

Langley Research Center
Hampton, VA 23681-0001

SUMMARY

A decoupled control approach for a Large Gap Magnetic Suspension System (LGMSS) is presented. The control approach is developed for an LGMSS which provides five-degree-of-freedom control of a cylindrical suspended element that contains a core composed of permanent magnet material. The suspended element is levitated above five electromagnets mounted in a planar array. Numerical results are obtained by using the parameters of the Large Angle Magnetic Suspension Test Fixture (LAMSTF) which is a small scale laboratory model LGMSS.

INTRODUCTION

This paper presents a decoupled, single-input single-output (SISO) control approach for a Large Gap Magnetic Suspension System (LGMSS). The control approach is developed for an LGMSS which provides five-degree-of-freedom control of a cylindrical suspended element that contains a core composed of permanent magnet material. The suspended element is levitated above five electromagnets mounted in a planar array. The LGMSS is a conceptual design for a ground-based experiment which could be used to investigate the technology issues associated with: magnetic suspension at large gaps, accurate suspended element control at large gaps, and accurate position sensing at large gaps (ref. 1). This technology would be applicable to future efforts which range from magnetic suspension of wind tunnel models to advanced spacecraft experiment isolation and pointing systems. An analytical model of an LGMSS configuration using five electromagnets mounted in a planar array is developed in reference 2. This model is used to investigate two LQR control approaches for the LGMSS in reference 3. In reference 3, the simplifying assumption is made that the change in field and field gradients with respect to suspended element displacements is negligible. In reference 4 the analytical model developed in reference 2 is linearized and extended to include the change in field and field gradients with respect to suspended element displacements and the open-loop characteristics of the resulting system are investigated. The purpose of this paper is to develop a decoupled SISO control approach for an LGMSS using the extended model developed in reference 4. The control approach is proportional-derivative (PD) where the command torques and forces are functions of positions and derivatives of position. Numerical results are obtained for a candidate design which uses parameters for a Large Angle Magnetic Suspension Test Fixture (LAMSTF). The LAMSTF was designed and built in order to investigate the feasibility of the LGMSS concept and to provide a test fixture for developing and demonstrating control approaches. Reference 5 presents a description of the LAMSTF and some of the control approaches which have been investigated. LAMSTF suspended element parameters and field components generated by the electromagnets at the centroid of the suspended element are presented in the Appendix.

SYMBOLS

$\mathcal{A}$	system matrix (state-space representation)
$\mathcal{B}$	input matrix (state-space representation)
$\tilde{\mathcal{B}}$	modified input matrix (eq. (13))
$\mathbf{B}$	magnetic flux density vector
$\mathbf{F}$	total force vector on suspended element
$\mathbf{F}_c$	command force vector
$\mathbf{G}$	gain matrix (eq. (59))
$\mathbf{G}_F$	forward-loop transfer function matrix (eq. (33))

g	acceleration due to gravity ($g \approx 9.81$ m/s^2)
h	suspension height, suspended element centroid to top plane of coils
$\mathbf{I}$	coil current vector
I_c	suspended element transverse moment of inertia
$\mathbf{K}$	coefficient matrix of field or field gradient components
KB_x, KB_y, KB_z	bias stiffness terms defined by equations (24), (25), and (26) respectively
$KB_{y\theta}$, $KB_{z\theta}$	bias stiffness terms defined by equation (22)
$KB_{y\theta x}$, $KB_{xy\theta}$	bias stiffness terms defined by equation (23)
KP_x, KR_x	position and rate gain for x control loop
KP_y, KR_y	position and rate gain for y control loop
KP_z, KR_z	position and rate gain for z control loop
$KP_{y\theta}$, $KR_{y\theta}$	position and rate gain for θ_y control loop
$KP_{z\theta}$, $KR_{z\theta}$	position and rate gain for θ_z control loop
$\mathbf{M}$	magnetization vector
m_c	suspended element mass
$\mathbf{T}$	total torque vector on suspended element
$\mathbf{T_c}$	command torque vector
$\mathbf{V}$	velocity vector
v	permanent magnet core volume
$\mathbf{W_1}$	weighting matrix (eq. (3))
x, y, z	coordinates in orthogonal axis system
x_c, y_c, z_c	position commands for x, y, z control loops respectively
ρ_x, ρ_y, ρ_z	damping ratio for x, y, z control loops respectively
$\rho_{y\theta}$, $\rho_{z\theta}$	damping ratio for θ_y and θ_z control loops respectively
θ	Euler orientation, 3, 2, 1 rotation sequence
θ_{yc}, θ_{zc}	position commands for θ_y and θ_z control loops respectively
$\mathbf{\Omega}$	rate of rotation
ω_x, ω_y, ω_z	natural frequency of x, y, z control loops respectively
$\omega_{y\theta}$, $\omega_{z\theta}$	natural frequency of θ_y and θ_z control loops respectively

Subscripts

b	electromagnet axes
ij	partial derivative of i component in j direction
$(ij)k$	partial derivative of ij partial derivative in k direction

max	maximum value
o	equilibrium condition
x, y, z	components along $x-$, $y-$, $z-$axes respectively
1–5	coil number

Matrix Notation

[ ]	matrix
$[\ ]^{-1}$	inverse of matrix
$[\ ]^T$	transpose of matrix
{ }	column vector
$\{\ \}^T$	transpose of column vector
⌊ ⌋	row vector

Dots over symbols denote derivatives with respect to time; a bar over a symbol indicates that it is referenced to suspended element coordinates.

EQUATIONS OF MOTION

The equations of motion for the LAMSTF are developed in this section using the linearized, extended, open-loop model of an LGMSS configuration consisting of five electromagnets mounted in a planar array which is presented in reference 4. Figure 1 is a schematic representation of the LAMSTF configuration which shows the coordinate systems and initial alignment. The suspended element coordinate system consists of a set of orthogonal $\bar{x}$, $\bar{y}$, $\bar{z}$ body-fixed axes which defines the motion of the suspended element with respect to inertial space. The suspended element coordinate system is initially aligned with an orthogonal x, y, z system fixed in inertial space. A set of orthogonal x_b, y_b, z_b axes, also fixed in inertial space, define the location of the electromagnet array with respect to the x, y, z system. The x_b and y_b axes are parallel to the x and y axes respectively and the z_b and z axes are aligned. The centers of the two axis systems are separated by the distance h. The open-loop equations of motion are of the form (ref. 2).

$$\dot{\mathbf{X}} = f(\mathbf{X}, \mathbf{u}) \tag{1}$$

where the state vector $\mathbf{X}$ is

$$\mathbf{X}^T = \lfloor \Omega_{\bar{y}}\ \Omega_{\bar{z}}\ \theta_y\ \theta_z\ V_{\bar{x}}\ V_{\bar{y}}\ V_{\bar{z}}\ x\ y\ z \rfloor \tag{2}$$

and the input vector u is

$$\mathbf{u}^T = \lfloor I_1 \quad I_2 \quad I_3 \quad I_4 \quad I_5 \rfloor \tag{3}$$

In reference 4 these equations are linearized around the nominal operating point $\mathbf{X}_o$, $\mathbf{I}_o$ by performing a Taylor series expansion. The linearized equations are (neglecting second-order terms and subtracting out $\dot{\mathbf{X}}_o$)

$$\delta\dot{\mathbf{X}} = \mathcal{A}\delta\mathbf{X} + \mathcal{B}\delta\mathbf{u} \tag{4}$$

where

$$\mathcal{A} = \partial\dot{\mathbf{X}}/\partial\mathbf{X}\Big|_{\mathbf{X}_o, \mathbf{I_o}} \tag{5}$$

and

$$\mathcal{B} = \partial\dot{\mathbf{X}}/\partial\mathbf{I}\Big|_{\mathbf{X}_o, \mathbf{I_o}} \tag{6}$$

From reference 4, $\mathcal{A}$ and $\mathcal{B}$ become

$$\mathcal{A} = vM_{\bar{x}}\mathbf{W}_1 \begin{bmatrix} 0 & 0 & -B_x & 0 & 0 & 0 & 0 & -B_{xz} & -B_{yz} & -B_{zz} \\ 0 & 0 & 0 & -B_x & 0 & 0 & 0 & B_{xy} & B_{yy} & B_{yz} \\ 1 & 0 & 0 & 0 & 0 & 0 & 0 & 0 & 0 & 0 \\ 0 & 1 & 0 & 0 & 0 & 0 & 0 & 0 & 0 & 0 \\ 0 & 0 & (m_c g - 2B_{xz}) & 2B_{xy} & 0 & 0 & 0 & B_{(xx)x} & B_{(xx)y} & B_{(xx)z} \\ 0 & 0 & -B_{yz} & (B_{yy} - B_{xx}) & 0 & 0 & 0 & B_{(xy)x} & B_{(xy)y} & B_{(xy)z} \\ 0 & 0 & (B_{xx} - B_{zz}) & B_{yz} & 0 & 0 & 0 & B_{(xz)x} & B_{(xz)y} & B_{(xz)z} \\ 0 & 0 & 0 & 0 & 1 & 0 & 0 & 0 & 0 & 0 \\ 0 & 0 & 0 & 0 & 1 & 0 & 0 & 0 & 0 & 0 \\ 0 & 0 & 0 & 0 & 0 & 0 & 1 & 0 & 0 & 0 \end{bmatrix} \tag{7}$$

$$\mathcal{B} = (vM_{\bar{x}}/I_{\max})\mathbf{W}_1 \begin{bmatrix} -\lfloor K_z \rfloor \\ \lfloor K_y \rfloor \\ \lfloor 0 \rfloor \\ \lfloor 0 \rfloor \\ \lfloor K_{xx} \rfloor \\ \lfloor K_{xy} \rfloor \\ \lfloor K_{xz} \rfloor \\ \lfloor 0 \rfloor \\ \lfloor 0 \rfloor \\ \lfloor 0 \rfloor \end{bmatrix} \tag{8}$$

where

$$\mathbf{W}_1 = \begin{bmatrix} 1/I_c & 0 & \cdot & \cdot & \cdot & & & & & 0 \\ 0 & 1/I_c & & & & & & & & \cdot \\ \cdot & & 1 & & & & & & & \cdot \\ \cdot & & & 1 & & & & & & \cdot \\ \cdot & & & & 1/m_c & & & & & \\ & & & & & 1/m_c & & & & \\ & & & & & & 1/m_c & & & \\ & & & & & & & 1 & & \\ & & & & & & & & 1 & \\ 0 & & \cdot & \cdot & \cdot & & & & & 1 \end{bmatrix} \tag{9}$$

The K coefficients in equation (8) represent the magnitude of field or field gradient components, at X_o, produced by a given current denoted $I_{\max}$. These components are presented in Tables A2

and A3 in the Appendix. For further discussion see reference 4. From reference 4 equation (52), the equilibrium value of B_{xz} is

$$B_{xz} = m_c g / v M_{\bar{x}} \tag{10}$$

Using the relationship of equation (10), element (5, 3) of the matrix in equation (7) reduces to

$$m_c g / v M \bar{x} - 2B_{xz} = -B_{xz} \tag{11}$$

Substituting this value in equation (7) and expanding equation (4) results in

$$I_c \dot{\Omega}_{\bar{y}} = v M_{\bar{x}} (-B_x \theta_y - B_{xz} x - B_{yz} y - B_{zz} z) + (v M_{\bar{x}} / I_{\max})(-\lfloor K_z \rfloor \{I\}) \tag{12}$$

$$I_c \dot{\Omega}_{\bar{z}} = v M_{\bar{x}} (-B_x \theta_z + B_{xy} x + B_{yy} y + B_{yz} z) + (v M_{\bar{x}} / I_{\max})(\lfloor K_y \rfloor \{I\}) \tag{13}$$

$$m_c \dot{V}_{\bar{x}} = v M_{\bar{x}} (-B_{xz} \theta_y + 2B_{xy} \theta_z + B_{(xx)x} x + B_{(xx)y} y + B_{(xx)z} z) + v M_{\bar{x}} / I_{\max}(\lfloor K_{xx} \rfloor \{I\}) \tag{14}$$

$$\begin{aligned} m_c \dot{V}_{\bar{y}} = {} & v M_{\bar{x}} (B_{yz} \theta_y + (B_{yy} - B_{xx}) \theta_z + B_{(xy)x} x + B_{(xy)y} y + B_{(xy)z} z) \\ & + v M_{\bar{x}} / I_{\max}(\lfloor K_{xy} \rfloor \{I\}) \end{aligned} \tag{15}$$

$$\begin{aligned} m_c \dot{V}_{\bar{z}} = {} & v M_{\bar{x}} ((B_{xx} - B_{zz}) \theta_y + B_{yz} \theta_z + B_{(xz)x} x + B_{(xz)y} y + B_{(xz)z} z) \\ & + v M_{\bar{x}} / I_{\max}(\lfloor K_{xz} \rfloor \{I\}) \end{aligned} \tag{16}$$

The first terms on the right in the above equations are the torques and forces generated on the core due to perturbations in X, evaluated in the presence of the uncontrolled fields and gradients produced by the constant or "bias" currents required to provide equilibrium suspension. The second terms are the torques and forces generated on the core by controlling the coil currents about the suspension currents. The controlled torques and forces can be written as

$$\begin{Bmatrix} \bar{T} \\ \bar{F} \end{Bmatrix} = [\widetilde{\mathcal{B}}] \{I\} \tag{17}$$

where

$$[\widetilde{\mathcal{B}}] = (v M_{\bar{x}}) / I_{\max} \begin{bmatrix} -\lfloor K_z \rfloor \\ \lfloor K_y \rfloor \\ \lfloor K_{xx} \rfloor \\ \lfloor K_{xy} \rfloor \\ \lfloor K_{xz} \rfloor \end{bmatrix} \tag{18}$$

From equation (17), the currents required to produce given command torques or forces become

$$\{I\} = [\widetilde{\mathcal{B}}]^{-1} \begin{Bmatrix} \overline{T} \\ \overline{F} \end{Bmatrix} \tag{19}$$

This decouples the forces and torques in terms of commands. As can be seen in equations (12)–(16) however, the motion is still highly coupled through the bias terms. In order to determine the extent of this coupling, the values for the bias, or uncontrolled field and gradient terms, can be calculated using the suspension currents as discussed in reference 4. The suspension currents, from equation (54) in reference 4, are

$$\{I_o\} = I_{\max} \begin{bmatrix} \lfloor K_y \rfloor \\ \lfloor K_z \rfloor \\ \lfloor K_{xx} \rfloor \\ \lfloor K_{xy} \rfloor \\ \lfloor K_{xz} \rfloor \end{bmatrix}^{-1} \begin{Bmatrix} 0 \\ 0 \\ 0 \\ 0 \\ B_{xz} \end{Bmatrix} \tag{20}$$

Using equation (10), with the suspended element parameters from the Appendix, the value of B_{xz} required for suspension is found to be 0.0965 T/m. With this value of B_{xz}, the currents required to provide equilibrium suspension were found to be (using eq. (20))

$$\{I_o\}^T = \lfloor -14.169 \quad -4.381 \quad 11.466 \quad 11.466 \quad -4.381 \rfloor \quad \text{(Amp.)} \tag{21}$$

These currents were then used to calculate the values of the bias fields and gradients. The results are presented in Table 1. Note that many of the terms are zero. Substituting these values into equations (12)–(16) and assuming that the control currents are generated by using equation (19) results in

$$\dot{\Omega}_{\bar{y}} = vM_{\bar{x}}/I_c(.0082\theta_y - .0965x) + (1/I_c)T_{yc} \tag{22}$$

$$\dot{\Omega}_{\bar{z}} = vM_{\bar{x}}/I_c(.0082\theta_z) + (1/I_c)T_{zc} \tag{23}$$

$$\dot{V}_{\bar{x}} = vM_{\bar{x}}/m_c(-.0965\theta_y + .4912x) + (1/m_c)F_{xc} \tag{24}$$

$$\dot{V}_{\bar{y}} = vM_{\bar{x}}/m_c(.9402y) + (1/m_c)F_{yc} \tag{25}$$

$$\dot{V}_{\bar{z}} = vM_{\bar{x}}/m_c(-.009z) + (1/m_c)F_{zc} \tag{26}$$

Since $B_{(xx)z}$ and $B_{(xz)x}$ are very small, they were neglected in equations (24) and (26). For simplification define

$$KB_{y\theta} = KB_{z\theta} = vM_{\bar{x}}(.0082) = .0184 \text{ Nm} \tag{27}$$

$$KB_{y\theta x} = KB_{xy\theta} = vM_{\bar{x}}(.0965) = .217 \text{ N} \tag{28}$$

$$KB_x = vM_{\bar{x}}(.4912) = 1.1048 \text{ N/m} \tag{29}$$

$$KB_y = vM_{\bar{x}}(.9402) = 2.1146 \text{ N/m} \tag{30}$$

$$KB_z = vM_{\bar{x}}(.009) = .0202 \text{ N/m} \tag{31}$$

Note that the positive bias terms in equations (22)–(26) cause open-loop instability. These terms are similar to the unstable bias flux stiffness terms encountered with small gap magnetic bearings which use permanent magnet bias flux (refs. 6 and 7). The positive bias terms in equations (22), (23), and (24) produce the unstable compass needle modes (modes 1 and 3) discussed in reference 4. Equations (22) and (24) are coupled through negative bias terms and this coupling produces the combined motion in modes 1 and 2. Mode 1, as mentioned, is unstable but mode 2 is a stable oscillatory mode. The positive bias term in equation (25) produces an unstable translation mode

(mode 5 in ref. 4). The negative bias term in equation (26) produces a stable oscillatory mode (mode 4 in ref. 4). The suspended element motions are uncoupled with the exception of pitch rotation (θ_y) and x translation (eqs. (22) and (24)). The open-loop eigenvalues are presented in Table 2.

CONTROL SYSTEM EQUATIONS

As mentioned earlier, the control approach is PD where the command torques and forces are functions of positions and derivatives of position. For PD control, the command torques and forces can be written as

$$T_{\bar{y}c} = (KP_{y\theta} + sKR_{y\theta})(\theta_{yc} - \theta_y) \tag{32}$$

$$T_{\bar{z}c} = (KP_{z\theta} + sKR_{z\theta})(\theta_{zc} - \theta_z) \tag{33}$$

$$F_{\bar{x}c} = (KP_x + sKR_x)(x_c - x) \tag{34}$$

$$F_{\bar{y}c} = (KP_y + sKR_y)(y_c - y) \tag{35}$$

$$F_{\bar{z}c} = (KP_z + sKR_z)(z_c - z) \tag{36}$$

where $KP_{y\theta}$, $KP_{z\theta}$, KP_x, KP_y, and KP_z are position gains for θ_y, θ_z, x, y, and z respectively, $KR_{z\theta}$, $KR_{y\theta}$, KR_x, KR_y, and KR_z are rate gains for $\dot{\theta}_y$, $\dot{\theta}_z$, $\dot{x}$, $\dot{y}$, and $\dot{z}$ respectively, θ_{yc}, θ_{zc}, x_c, y_c, and z_c are position commands, and s is the Laplace operator. A block diagram of this control system is presented in figure 2.

Control of pitch rotation (θ_y) and x translation will be examined first since these are the only suspended element motions which are coupled. The approach is to close control loops around each axis independently and to determine the effect of the cross-coupling on the design of the individual loops. In matrix form, (32) and (34) can be written as

$$\begin{Bmatrix} T_{\bar{y}c} \\ F_{\bar{x}c} \end{Bmatrix} = [G_F] \begin{Bmatrix} (\theta_{yc} - \theta_y) \\ (x_c - x) \end{Bmatrix} \tag{37}$$

where $[G_F]$ is a forward-loop transfer function matrix defined as

$$[G_F] = \begin{bmatrix} (KP_{y\theta} + sKR_{y\theta} & 0 \\ 0 & (KP_x + sKR_x) \end{bmatrix} \tag{38}$$

Taking the Laplace transform of equations (22) and (24) and putting them in matrix form results in

$$\begin{Bmatrix} s^2\theta_y \\ s^2x \end{Bmatrix} = \begin{bmatrix} (1/I_c)KB_{y\theta} & -(1/I_c)KB_{y\theta x} \\ -(1/m_c)KB_{y\theta x} & (1/m_c)KB_x \end{bmatrix} \begin{Bmatrix} \theta_y \\ x \end{Bmatrix} + \begin{Bmatrix} (1/I_c)T_{\bar{y}c} \\ (1/m_c)F_{\bar{x}c} \end{Bmatrix} \tag{39}$$

Substituting for $T_{\bar{y}c}$ and $F_{\bar{x}c}$ in (39) and collecting terms results in

$$\begin{bmatrix} (I_cs^2 + KR_{y\theta}s + (KP_{y\theta} - KB_{y\theta})) & KB_{y\theta x} \\ KB_{y\theta x} & (m_cs^2 + KR_xs + (KP_x - KB_x)) \end{bmatrix} \begin{Bmatrix} \theta_y \\ x \end{Bmatrix} = [\mathrm{G_F}] \begin{Bmatrix} \theta_{yc} \\ x_c \end{Bmatrix} \tag{40}$$

The characteristic equation becomes

$$\det \begin{vmatrix} (I_cs^2 + KR_{y\theta}s + (KP_{y\theta} - KB_{y\theta})) & KB_{y\theta x} \\ KB_{y\theta x} & (m_cs^2 + KR_xs + (KP_x - KB_x)) \end{vmatrix} = 0 \tag{41}$$

Expanding the determinant results in

$$(s^2 + KR_{y\theta}s/I_c + (KP_{y\theta} - KB_{y\theta})/I_c)(s^2 + KR_x s/m_c + (KP_x - KB_x)/m_c) - KB^2_{y\theta x}/I_c m_c = 0 \quad (42)$$

The natural frequency of the θ_y control loop, independent of the cross coupling, becomes

$$\omega_{y\theta} = \sqrt{(KP_{y\theta} - KB_{y\theta})/I_c} \quad (43)$$

with a damping ratio of

$$\rho_{y\theta} = KR_{y\theta}/(2\sqrt{(KP_{y\theta} - KB_{y\theta})I_c}) \quad (44)$$

Similarly for the x control loop

$$\omega_x = \sqrt{(KP_x - KB_x)/m_c} \quad (45)$$

and

$$\rho_x = KR_x/(2\sqrt{(KP_x - KB_x)m_c}) \quad (46)$$

The cross coupling term, $KB^2_{y\theta x}/I_c m_c$, can be defined as an equivalent natural frequency

$$\omega_c = KB_{y\theta x/}(\sqrt{I_c m_c}) \quad (47)$$

Substituting (43)–(47) into (42) and expanding results in

$$\begin{aligned} s^4 + (2\rho_{y\theta}\omega_{y\theta} + 2\rho_x\omega_x)s^3 + ((2\rho_{y\theta}\omega_{y\theta})(2\rho_x\omega_x) + \omega^2_{y\theta} + \omega^2_x)s^2 \\ + ((2\rho_{y\theta}\omega_{y\theta})(\omega^2_x) + (2\rho_x\omega_x)(\omega^2_{y\theta}))s + \omega^2_{y\theta}\omega^2_x - \omega^2_c = 0 \end{aligned} \quad (48)$$

The characteristic equations for the remaining, uncoupled, control loops can be obtained in a similar manner. For yaw rotation (θ_z), y, and z translation respectively, the characteristic equations become

$$s^2 + KR_{z\theta}s/I_c + (KP_{z\theta} - KB_{z\theta})/I_c = 0 \quad (49)$$

$$s^2 + KR_y s/m_c + (KP_y - KB_y)/m_c = 0 \quad (50)$$

$$s^2 + KR_z s/m_c + (KP_z - KB_z)/m_c = 0 \quad (51)$$

Damping ratios and natural frequencies become

$$\rho_{z\theta} = KR_{z\theta}/(2\sqrt{(KP_{z\theta} - KB_{z\theta})I_c}) \quad (52)$$

$$\omega_{z\theta} = \sqrt{(KP_{z\theta} - KB_{z\theta})}/I_c \quad (53)$$

$$\rho_y = KR_y/(2\sqrt{(KP_y - KB_y)m_c}) \quad (54)$$

$$\omega_y = \sqrt{(KP_y - KB_y)/m_c} \quad (55)$$

$$\rho_z = KR_z/(2\sqrt{(KP_z - KB_z)m_c}) \quad (56)$$

$$\omega_z = \sqrt{(KP_z - KB_z)/m_c} \quad (57)$$

EXAMPLE DESIGN

In order to investigate the effects of the cross-coupling discussed earlier, consider an example design where the natural frequency of each loop is set to 100 rad/sec and the damping ratio is set to 0.7. Using equations (43)–(47) and (52)–(57), the rate gains and position gains become

$$KR_{y\theta} = KR_{z\theta} = 7.7126(10)^{-4} \text{ Nms/rad} \tag{58}$$

$$KR_x = KR_y = KR_z = 3.0974 \text{ Ns/m} \tag{59}$$

$$KP_{y\theta} = KPz_\theta = 0.0735 \text{ Nm/rad} \tag{60}$$

$$KP_x = 222.3447 \text{ N/m} \tag{61}$$

$$KP_y = 223.3545 \text{ N/m} \tag{62}$$

$$KP_z = 221.2601 \text{ N/m} \tag{63}$$

For simplicity, assume a zero set-point and perfect differentiators. The command torques and forces can then be written as

$$\begin{Bmatrix} T_{\bar{y}c} \\ T_{\bar{z}c} \\ F_{\bar{x}c} \\ F_{\bar{y}c} \\ F_{\bar{z}c} \end{Bmatrix} = \begin{bmatrix} KR_{y\theta} & 0 & KP_{y\theta} & 0 & 0 & 0 & 0 & 0 & 0 & 0 \\ 0 & KR_{z\theta} & 0 & KR_{z\theta} & 0 & 0 & 0 & 0 & 0 & 0 \\ 0 & 0 & 0 & 0 & KR_x & 0 & 0 & KP_x & 0 & 0 \\ 0 & 0 & 0 & 0 & 0 & KR_y & 0 & 0 & KP_y & 0 \\ 0 & 0 & 0 & 0 & 0 & 0 & KR_z & 0 & 0 & KP_z \end{bmatrix} \{X\} \tag{64}$$

or, using compact notation

$$\begin{Bmatrix} \overline{T}_c \\ \overline{F}_c \end{Bmatrix} = -[G]\{X\} \tag{65}$$

The current becomes, from equation (19)

$$\{I\} = [\tilde{\mathcal{B}}]^{-1}[G]\{X\} \tag{66}$$

Substituting for u in equation (3) results in

$$\dot{X} = (A - \mathcal{B}\tilde{\mathcal{B}}^{-1}G)X \tag{67}$$

The eigenvalues of $(A - \mathcal{B}\tilde{\mathcal{B}}^{-1}G)$ are presented in Table 2. The first two sets are related to the coupled axes (pitch rotation and x translation). The damping ratios and natural frequencies of these eigenvalues differ from the design values by approximately three percent. The same values are obtained by finding the roots of equation (43). Position and rate gains for pitch rotation and x translation can be independently varied to adjust the coupled damping ratios and natural frequencies. Varying these gains have no effect on the remaining eigenvalues.

CONCLUDING REMARKS

A decoupled, SISO, control approach for an LGMSS has been presented. The control approach is for an LGMSS which provides five-degree-of-freedom control of a cylindrical suspended element that contains a core composed of permanent magnet material. The control approach decouples the

five degrees of freedom in terms of force and torque commands. However, the pitch rotation and x translation axes remain coupled through bias terms resulting from the bias currents required to produce equilibrium suspension. Equations for position and rate gains for each axis are developed in terms of natural frequencies and damping ratios. In order to investigate the effects of pitch rotation and x translation coupling, an example design was performed using the parameters of the Large Angle Magnetic Suspension Test Fixture (LAMSTF) which is a small scale laboratory model LGMSS. Results of the design indicated that the damping ratios and natural frequencies of the coupled axes differed from design values but not by a significant amount (approximately three percent for the design considered).

APPENDIX
LARGE ANGLE MAGNETIC SUSPENSION SYSTEM (LAMSTF) PARAMETERS

This appendix presents, in the form of tables, LAMSTF suspended-element, permanent magnet core, and electromagnet parameters and components of fields and gradients (including second-order gradients) generated by the LAMSTF electromagnets at the centroid of the suspended element. The LAMSTF contains a planar array of five room-temperature electromagnets, with iron cores, mounted in a circular configuration. The configuration is shown schematically in figure 1. For a more detailed description of the LAMSTF see reference 5. The fields and gradients were calculated using VF/GFUN (ref. 8), including the pre- and post-processor OPERA, with all iron cores modelled. LAMSTF parameters are presented in Table A1. Electromagnet fields and first-order gradients are presented in Table A2 and second-order gradients are presented in Table A3. It should be noted that the full set of components is not included in the tables since $B_{(ij)} = B_{(ji)}$ and $B_{(ij)k} = B_{(ik)j} = B_{(jk)i}$.

Table A1. LAMSTF Parameters

Core diameter, m	$8.509(10)^{-3}$
Core length, m	$5.08(10)^{-2}$
Suspended element mass (m_c), kg	$22.124(10)^{-3}$
Suspended element inertia (I_c), $kg - m^2$	$5.508(10)^{-6}$
Core volume (v), m^3	$2.889(10)^{-6}$
Core magnetization (M_x), A/m	$7.785(10)^5$
Suspended element suspension height (h), m	0.1
Electromagnet outer radius, m	0.0825
Electromagnet inner radius, m	0.0475
Electromagnet height, m	0.105
Iron core radius, m	0.038
Location radius*, m	0.1375
I_{max}, A	10.0

*Distance from center of array to axis of given coil.

Table A2. Electromagnet Fields and First-Order Gradients
Calculated at Nominal Suspension Location

	B_x	B_y	B_z	B_{xx}	B_{xy}	B_{xz}	B_{yy}	B_{yz}	B_{zz}
Electromagnet	(Tesla)			(Tesla/meter)					
1	+.0023	0	−.0009	+.0218	0	−.0272	−.0189	0	−.0029
2	+.0007	+.0022	−.0009	−.0150	+.0120	−.0084	+.0179	−.0259	−.0029
3	−.0019	+.0014	−.0009	+.0077	−.0194	+.0220	−.0049	−.0160	−.0029
4	−.0019	−.0014	−.0009	+.0077	+.0194	+.0220	−.0049	+.0160	−.0029
5	+.0007	−.0022	−.0009	−.0150	−.0120	−.0084	+.0179	+.0259	−.0029

All values calculated for $I_{\max} = 10$ Amp.

Table A3. Electromagnet Second-Order Gradients
Calculated at Nominal Suspension location

	$B_{(xx)x}$	$B_{(xy)x}$	$B_{(xz)x}$	$B_{(xy)y}$	$B_{(xy)z}$	$B_{(xz)z}$
Electromagnet	(Tesla/meter/meter)					
1	+.0343	0	−.5347	−.2192	0	+.0025
2	−.1828	−.1456	+.1637	−.1194	+.0874	+.0008
3	+.1656	+.1373	−.2679	+.2290	−.1413	−.0021
4	+.1656	−.1373	−.2679	+.2290	+.1413	−.0021
5	−.1828	+.1456	+.1637	−.1194	−.0874	+.0008

All values calculated for $I_{\max} = 10$ Amp.

REFERENCES

1. Groom, Nelson J.: Description of the Large Gap Magnetic Suspension System (LGMSS) Ground-Based Experiment. NASA CP-3109, Vol. 2, March 1991, pp. 365–377.
2. Groom, Nelson J.: Analytical Model Of A Five Degree Of Freedom Magnetic Suspension And Positioning System. NASA TM-100671, March 1989.
3. Groom, Nelson J. and Schaffner, Philip R.: An LQR Controller Design Approach for a Large Gap Magnetic Suspension System (LGMSS). NASA TM-101606, July 1990.
4. Groom, Nelson J. and Britcher, Colin P.: Open-Loop Characteristics of Magnetic Suspension Systems Using Electromagnets Mounted in a Planar Array. NASA TP-3229, November 1992.
5. Groom, Nelson J. and Britcher, Colin P.: A Description of a Laboratory Model Magnetic Suspension Test Fixture with Large Angular Capability. Proceedings of The First IEEE Conference on Control Applications, September 13–16 1992, Dayton, OH, Vol. 1, pp. 454–459.
6. Groom, Nelson J.: Analytical Model Of An Annular Momentum Control Device (AMCD) Laboratory Test Model Magnetic Bearing Actuator. NASA TM-80099, August 1979.
7. Groom, Nelson J., Woolley, Charles T. and Joshi, Suresh M.: Analysis and Simulation of a Magnetic Bearing Suspension System for a Laboratory Model Annular Momentum Control Device. NASA TP-1799, March 1981.
8. The VF/GFUN Reference Manual. VF068894, Vector Fields Limited, June 20, 1988.

Table 1. Bias Fields and Gradients

B_x, Tesla	−0.0082
B_{xx}, Tesla/meter	0
B_{xy}, Tesla/meter	0
B_{xz}, Tesla/meter	0.0965
B_{yy}, Tesla/meter	0
B_{yz}, Tesla/meter	0
B_{zz}, Tesla/meter	0
$B_{(xx)x}$, Tesla/meter/meter	0.4912
$B_{(xx)y}$, Tesla/meter/meter	0
$B_{(xx)z}$, Tesla/meter/meter	0.0002
$B_{(xy)x}$, Tesla/meter/meter	0
$B_{(xy)y}$, Tesla/meter/meter	0.9402
$B_{(xy)z}$, Tesla/meter/meter	0
$B_{(xz)x}$, Tesla/meter/meter	0.0002
$B_{(xz)y}$, Tesla/meter/meter	0
$B_{(xz)z}$, Tesla/meter/meter	−0.009

Table 2. System Eigenvalues for Example Design

Open-loop Eigenvalues	Damping Ratio (ρ)	Natural Frequency (ω_n)
+/−58.77	Unstable	58.77
+/−7.97i	0	7.97
+/−57.8	Unstable	57.8
+/−0.96i	0	0.96
+/−9.78	Unstable	9.78

Closed-loop Eigenvalues	Damping Ratio (ρ)	Natural Frequency (ω_n)
−70.01+/−75.64i	0.68	103.1
−70.01+/−66.92i	0.72	96.8
−70.01+/−71.42i	0.7	100
−70.00+/−71.43i	0.7	100
−70.00+/−71.41i	0.7	100

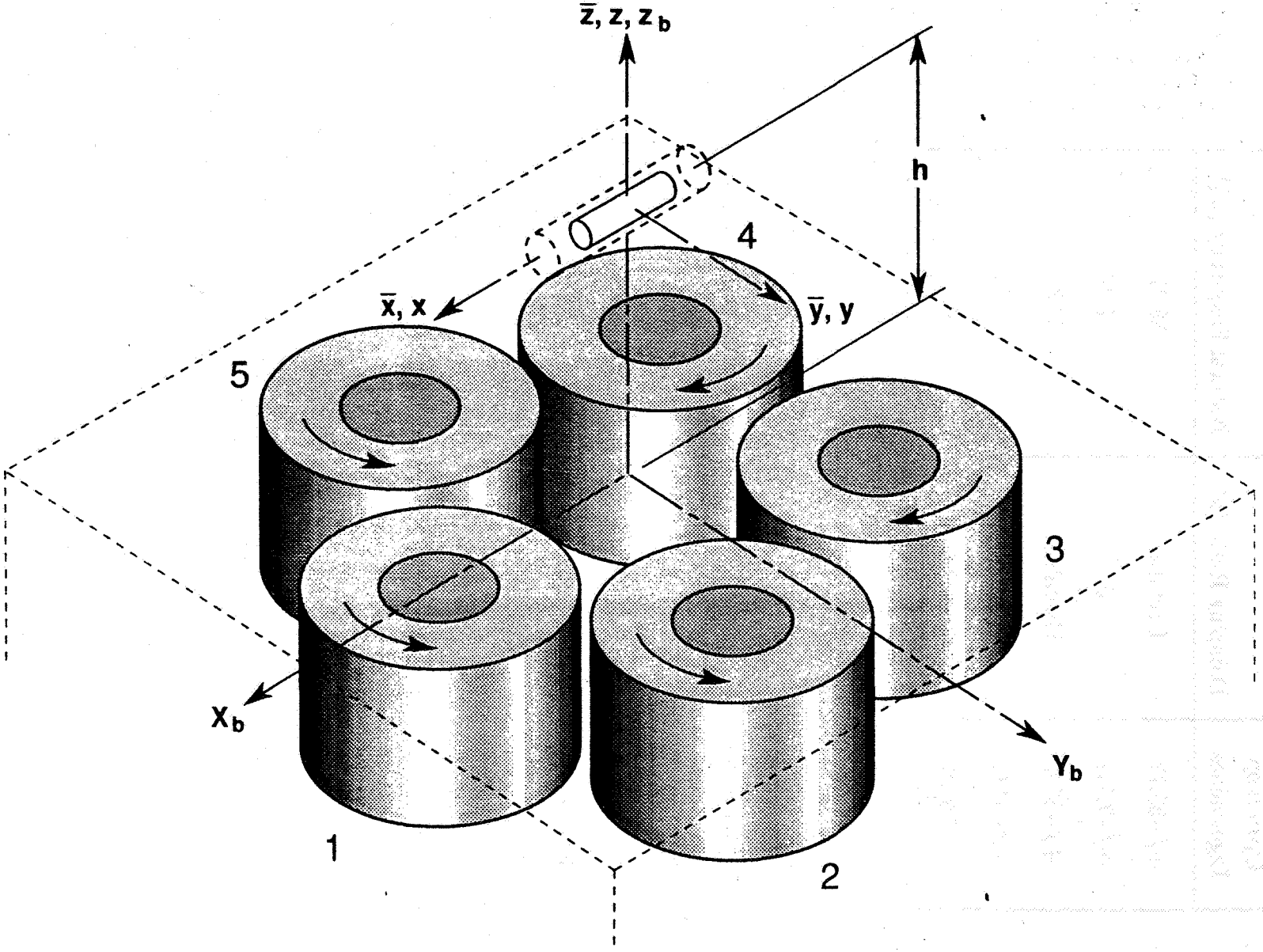

Figure 1. - LAMSTF Configuration

109.1213.001.106.A

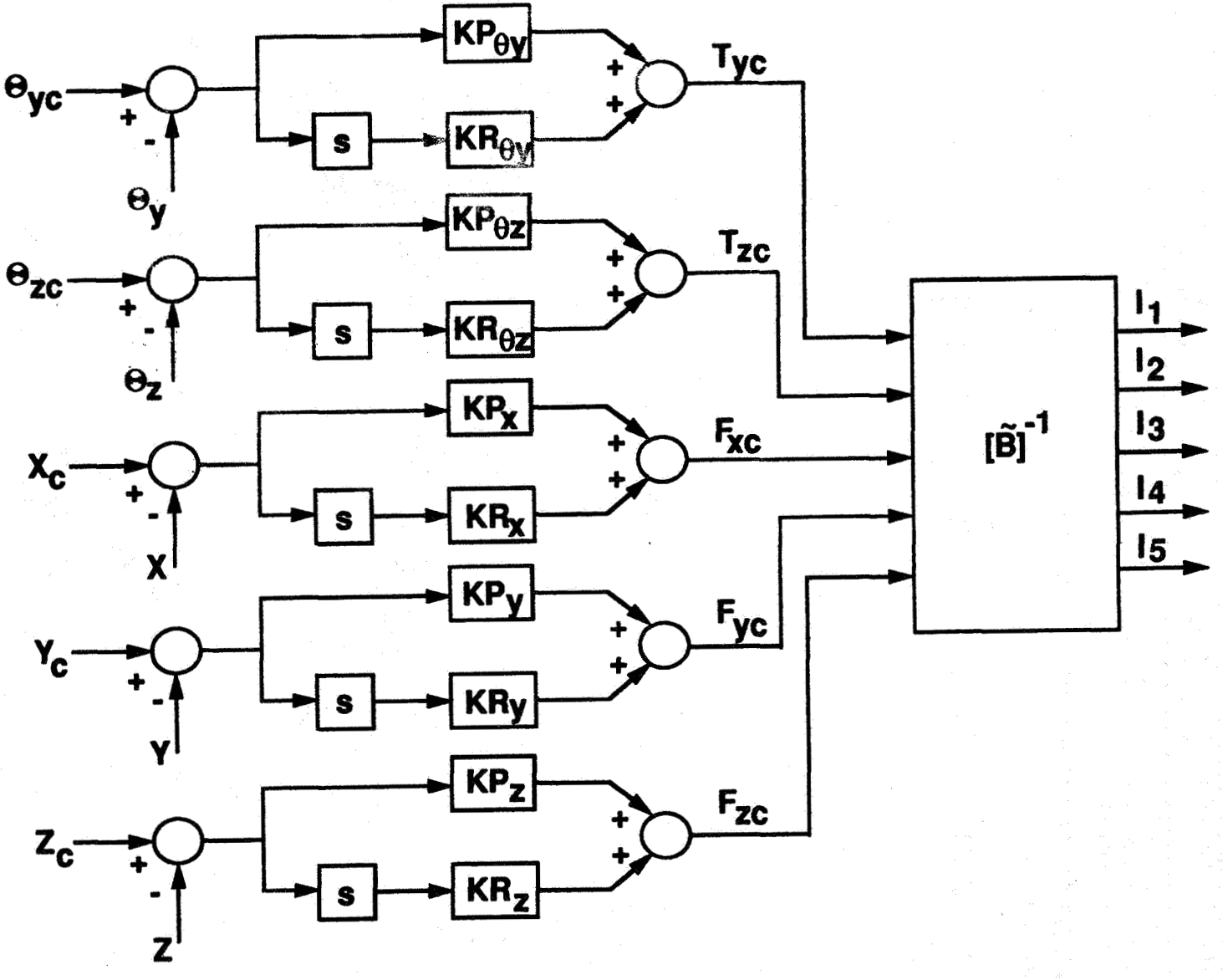

Figure 2. - Block Diagram of Decoupled Single-Input Single-Output Control System.

REPORT DOCUMENTATION PAGE

Form Approved
OMB No. 0704-0188

1. AGENCY USE ONLY *(Leave blank)*	2. REPORT DATE	3. REPORT TYPE AND DATES COVERED
	August 1993	Technical Memorandum

4. TITLE AND SUBTITLE
A Decoupled Control Approach for Magnetic Suspension Systems Using Electromagnets Mounted in a Planar Array

5. FUNDING NUMBERS
WU 506-59-61-05

6. AUTHOR(S)
Nelson J. Groom

7. PERFORMING ORGANIZATION NAME(S) AND ADDRESS(ES)
NASA Langley Research Center
Hampton, VA 23681-0001

8. PERFORMING ORGANIZATION REPORT NUMBER

9. SPONSORING/MONITORING AGENCY NAME(S) AND ADDRESS(ES)
National Aeronautics and Space Administration
Washington, DC 20546-0001

10. SPONSORING/MONITORING AGENCY REPORT NUMBER
NASA TM-109011

11. SUPPLEMENTARY NOTES

12a. DISTRIBUTION/AVAILABILITY STATEMENT
Unclassified–Unlimited
Subject Category 31

12b. DISTRIBUTION CODE

13. ABSTRACT *(Maximum 200 words)*

A decoupled control approach for a Large Gap Magnetic Suspension System (LGMSS) is presented. The control approach is developed for an LGMSS which provides five degree-of-freedom control of a cylindrical suspended element that contains a core composed of permanent magnet material. The suspended element is levitated above five electromagnets mounted in a planar array. Numerical results are obtained by using the parameters of the Large Angle Magnetic Suspension Test Fixture (LAMSTF) which is a small scale laboratory model LGMSS.

14. SUBJECT TERMS
Magnetic Suspension; Large-Gap Magnetic Suspension; Magnetic Levitation; Magnetic Suspension Model; Planar Array Suspension Coils; Decoupled Control

15. NUMBER OF PAGES
18

16. PRICE CODE
A03

17. SECURITY CLASSIFICATION OF REPORT	18. SECURITY CLASSIFICATION OF THIS PAGE	19. SECURITY CLASSIFICATION OF ABSTRACT	20. LIMITATION OF ABSTRACT
Unclassified	Unclassified	Unclassified	UL